Effects of magnetic ordering on Raman scattering spectra of Bi_2CuO_4

1994 J. Phys.: Condens. Matter 6 10357

(http://iopscience.iop.org/0953-8984/6/47/018)

J. Phys.: Condens. Matter 6 (1994) 10357–10363. Printed in the UK

Effects of magnetic ordering on Raman scattering spectra of Bi_2CuO_4

M J Konstantinović and Z V Popović
Institute of Physics, PO Box 57, 11000 Belgrade, Yugoslavia

Received 10 April 1994

Abstract. In the present study, Raman scattering selection rules for different spin orientation in Bi_2CuO_4 are compared with polarized Raman scattering spectra. This comparison suggests z-axis orientation of magnetic moments. The temperature dependence of phonon modes is studied and strong spin-dependent behaviour near the Néel temperature is shown for A_{1g} symmetry modes.

1. Introduction

The discovery of the high-temperature oxides induced a huge interest in investigation of different properties of Cu–O-based materials. Bi_2CuO_4 is one of the possible 'impurity phases' in the Bi–Sr–Ca–Cu–O system. This crystal has a tetragonal structure (space group $P4/ncc$) with isolated CuO_4 square-planar units of Cu^{2+} ions, which are stacked one on top of another in a staggered manner along the c axis. The bismuth atoms are connected to CuO_4 planes through the $(BiO_2)_n$ chains along the c axis. The description of the Bi_2CuO_4 crystal structure can be found in [1]. Bi_2CuO_4 crystal orders antiferromagnetically below $T_N = 45$ K. There is some controversy about magnetic moment orientation. In [2–3], it is stated that spins are oriented along the z axis while the recent paper [4] shows x-axis orientation of magnetic moments. Spin waves in Bi_2CuO_4 were analysed using Raman [5] and neutron [6] spectroscopy. In [5], one- and two-magnon modes as well as their polarization and temperature dependencies are shown. A neutron scattering study shows four different Cu–O–Bi–O–Cu pathways through which superexchange propagates and consequently four superexchange constants, necessary to fit the magnon dispersion experimental data, are obtained [6].

The vibrational properties of this compound were studied by us previously, using infrared and Raman spectroscopy as well as lattice dynamical calculation [7, 8].

In the present study, Raman scattering selection rules for different spin orientation in Bi_2CuO_4 are compared with polarized Raman scattering spectra. This comparison suggests z-axis orientation of magnetic moment. Nevertheless, the temperature dependences of phonon modes are presented and strong spin-dependent behaviour near the Néel temperature is shown for A_{1g} symmetry modes.

2. Experimental details

The growth of Bi_2CuO_4 single crystals was carried out by a floating-zone technique associated with an ellipsoidal image furnace [9]. The Raman spectra were measured using a Jobin Yvon monochromator model U-1000 with 1800 grooves mm^{-1} holographic gratings.

0953-8984/94/4710357+07$19.50

The 514.5 nm line of an argon ion laser (the average power was about 100 mW) was used as excitation source. As a detector, we used a Pelletier-effect-cooled RCA 31034A photomultiplier with a conventional photon-counting system. The samples were held in a closed-cycle cryostat.

3. Results and discussion

The polarized Raman spectra of the Bi_2CuO_4 single crystal from the (001) and the $(1\bar{1}0)$ plane were measured in the spectral range between 10 and 650 cm^{-1} at different temperatures, and presented in figure 1. Factor group analysis predicts $5A_{1g}+4B_{2g}+5B_{1g}+11E_g$ Raman active modes [8]. All A_{1g} and B_{2g} Raman active modes were observed in the $y'(zz)\bar{y}'$ (figure 1(*a*)) and the $z(xy)\bar{z}$ (figure 1(*c*)) configurations, respectively. The $y'(x'z)\bar{y}'$ and $z(x'y')\bar{z}$ polarized spectra with E_g and B_{1g} Raman active modes are shown in figure 1(*b*) and figure 1(*d*), respectively. The polarized spectra with the $z(xx)\bar{z}$ configuration, as shown in figure 1(*d*) includes A_{1g} and B_{1g} symmetry modes. Figure 1(*f*) shows Raman scattering spectra of the $z(x'x')\bar{z}$ configuration which contains A_{1g} and B_{2g} symmetry modes. The assignment of these phonon modes is given earlier [8] and we will not discuss them here.

One wide feature becomes dominant below $T_N = 45$ K, (see figure 1(*b*), (*d*) and (*e*)). We assigned it as a two-magnon mode [5]. The small peak denoted by the arrow in figure 1(*b*) comes from one-magnon scattering, as was already discussed in [5].

As we previously mentioned, two directions of the magnetic moments are proposed. We will therefore discuss further Raman scattering selection rules from two possible magnetic space groups and compare our spectra with these predictions. In the first case we consider the crystal structure with spin along the x axis in antiferromagnetic phase. Below the Néel temperature, the x direction is no longer equivalent to the y direction, and the symmetry of the crystal structure is reduced from tetragonal to orthorhombic. From symmetry operation analysis, including the time reversal operation, we obtain the magnetic point group mmm', $D_{2h}(C_{2v})$ (the unitary subgroup is shown in parentheses). For the spins along the z axis, the second case, the crystal structure remains tetragonal and the magnetic point group is $4/m'm'm'$, $D_{4h}(D_4)$. Corresponding magnetic space groups for above two cases are $Pnnm'$ (C_{2v}^3) and $P4/n'c'c'$ (D_4^2). Following the work of Cracknell [10] the magnetic Raman tensors of these two groups are:

mmm'

$$\begin{array}{ll} \mathrm{DA}\ \mathrm{D}\Gamma_1^1 \begin{pmatrix} \mathrm{A} & & \\ & \mathrm{E} & \\ & & \mathrm{I} \end{pmatrix} & \mathrm{DA}\ \mathrm{D}\Gamma_2^2 \begin{pmatrix} & & \mathrm{B} \\ \mathrm{D} & & \end{pmatrix} \\ \mathrm{DB}\ \mathrm{D}\Gamma_3^2 \begin{pmatrix} & & \mathrm{C} \\ & \mathrm{G} & \end{pmatrix} & \mathrm{DB}\ \mathrm{D}\Gamma_4^2 \begin{pmatrix} & & \\ & & \mathrm{F} \\ & \mathrm{H} & \end{pmatrix} \end{array} \tag{1}$$

$4/m'm'm'$

$$\begin{array}{ll} \mathrm{DA}\ \mathrm{D}\Gamma_1^1 \begin{pmatrix} \mathrm{A} & & \\ & \mathrm{A} & \\ & & \mathrm{I} \end{pmatrix} & \mathrm{DA}\ \mathrm{D}\Gamma_2^2 \begin{pmatrix} & & \mathrm{B} \\ -\mathrm{B} & & \end{pmatrix} \\ \mathrm{DB}\ \mathrm{D}\Gamma_3^1 \begin{pmatrix} \mathrm{E} & & \\ & -\mathrm{E} & \end{pmatrix} & \mathrm{DB}\ \mathrm{D}\Gamma_4^2 \begin{pmatrix} & & \mathrm{D} \\ \mathrm{D} & & \end{pmatrix} \\ \mathrm{DE}\ \mathrm{D}\Gamma_5 \left\langle \begin{pmatrix} & & \\ & & \mathrm{F} \\ & \mathrm{H} & \end{pmatrix} \begin{pmatrix} & & -\mathrm{F} \\ & -\mathrm{H} & \end{pmatrix} \right\vert . & \end{array} \tag{2}$$

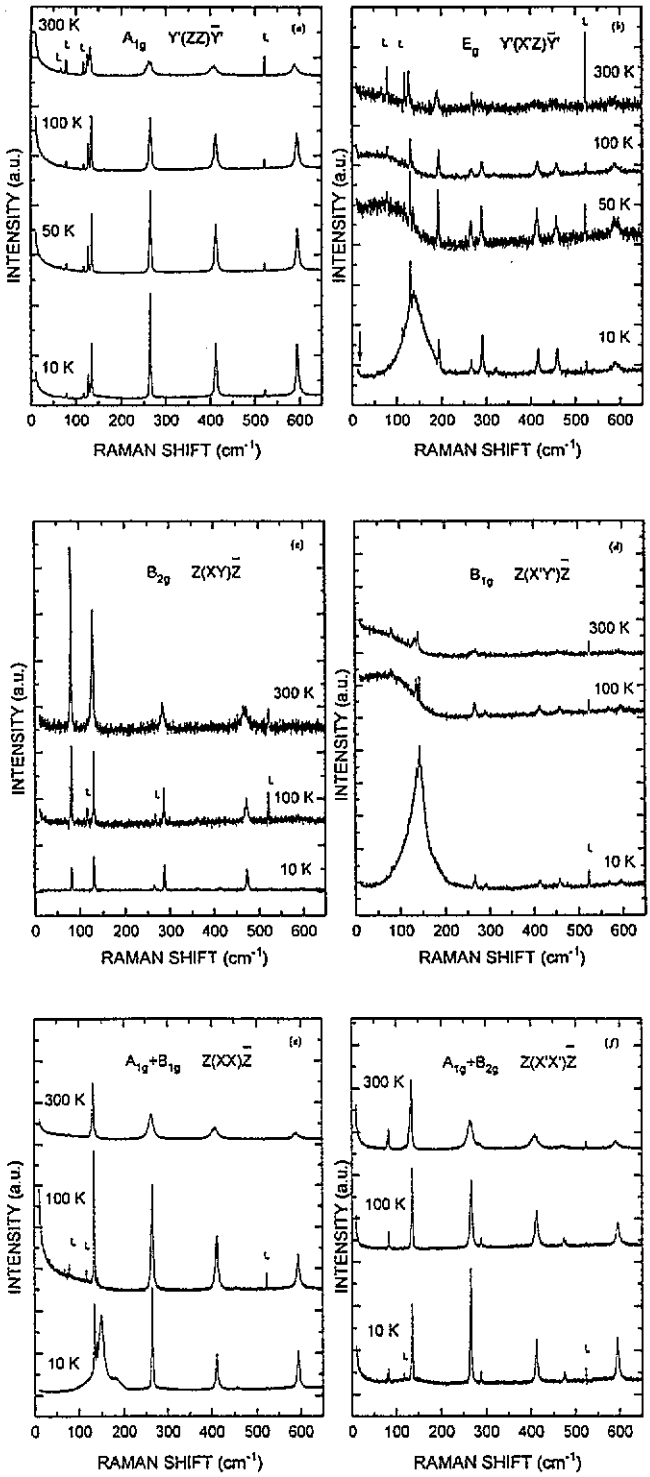

Figure 1. Raman scattering spectra of Bi_2CuO_4 single crystal at various temperatures for (*a*) $y'(zz)\bar{y}'$ (*b*) $y'(x'z)\bar{y}'$ (*c*) $z(xy)\bar{z}$ (*d*) $z(x'y')\bar{z}$ (*e*) $z(xx)\bar{z}$ and (*f*) $z(x'x')\bar{z}$ polarizations. (L denotes plasma lines and $x\|[100]$, $y\|[010]$, $z\|[001]$, $x'\|[110]$, $y'\|[1\bar{1}0]$).

Considering the symmetry through the whole Brillouin zone and Raman tensors listed above, we concluded that the spin orientation is more likely along the z direction due to the following arguments.

(i) At the Γ point, the spin wave will transform as $S_x \pm iS_y$ (spin along the z axis) which belong to the corepresentation DE ($D\Gamma_5$) of the group D_4^2. It follows that the spin-wave spectra are doubly degenerate which indeed has been observed [4, 6]. Furthermore, the one-magnon excitation gives contributions in the xz and yz polarization configurations in agreement with our spectra [5].

(ii) For the two-magnon excitation there are additional selection rules that apply at the special points of symmetry. Using the standard procedure [11] we obtained the symmetry of the two-magnon state at the different symmetry points assigned to the appropriate corepresentation at Γ. At the Z point the two-magnon state transform as DB_1 ($D\Gamma_3$); X and R are points with the same symmetry and the two-magnon process is active in DB_1 ($D\Gamma_3$) and DE ($D\Gamma_5$) corepresentation; M and A points are also degenerate due to the high symmetry of the unit cell but they give no contribution to the two-magnon spectra. From Raman tensors, equation (2), it follows that the two-magnon excitation should be observed in xx, $x'y'$ and $x'z$ polarized configuration, which is in excellent agreement with our results, figure 1.

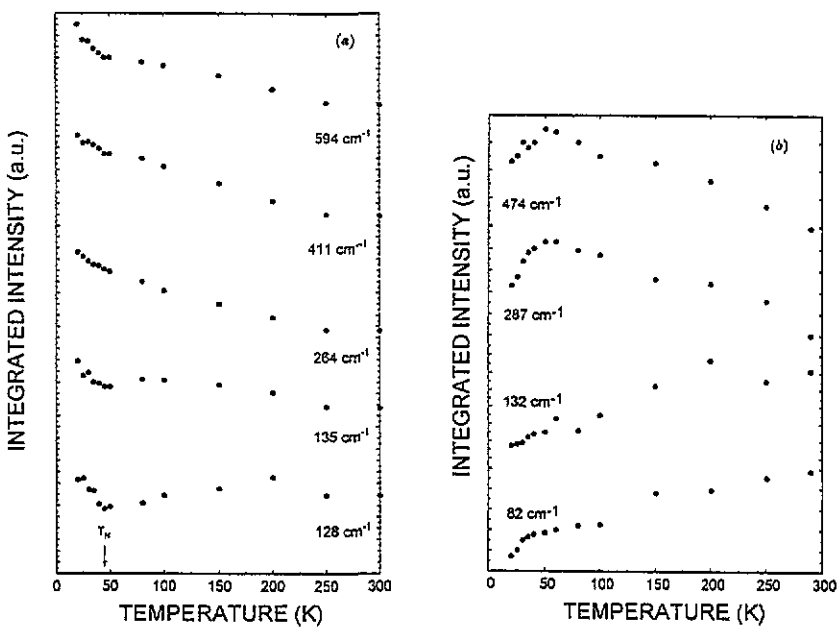

Figure 2. Integrated intensities of the A_{1g} (*a*) and B_{2g} (*b*) phonon modes as functions of the temperature.

(iii) The spin orientation along x axis did not predict degeneration of spin wave spectra at Γ. The Raman tensors, equation (1) allow observation of the one-magnon mode in yz and xy polarized configuration. Finally, the selection rules of the orthorhombic space group indicates that the two-magnon excitation could not explain the activity of two-magnon in xx and inactivity in $x'x'$ and zz polarizations. All in all, the polarized Raman scattering spectra given in figure 1 show z-axis orientation of magnetic moments in Bi_2CuO_4.

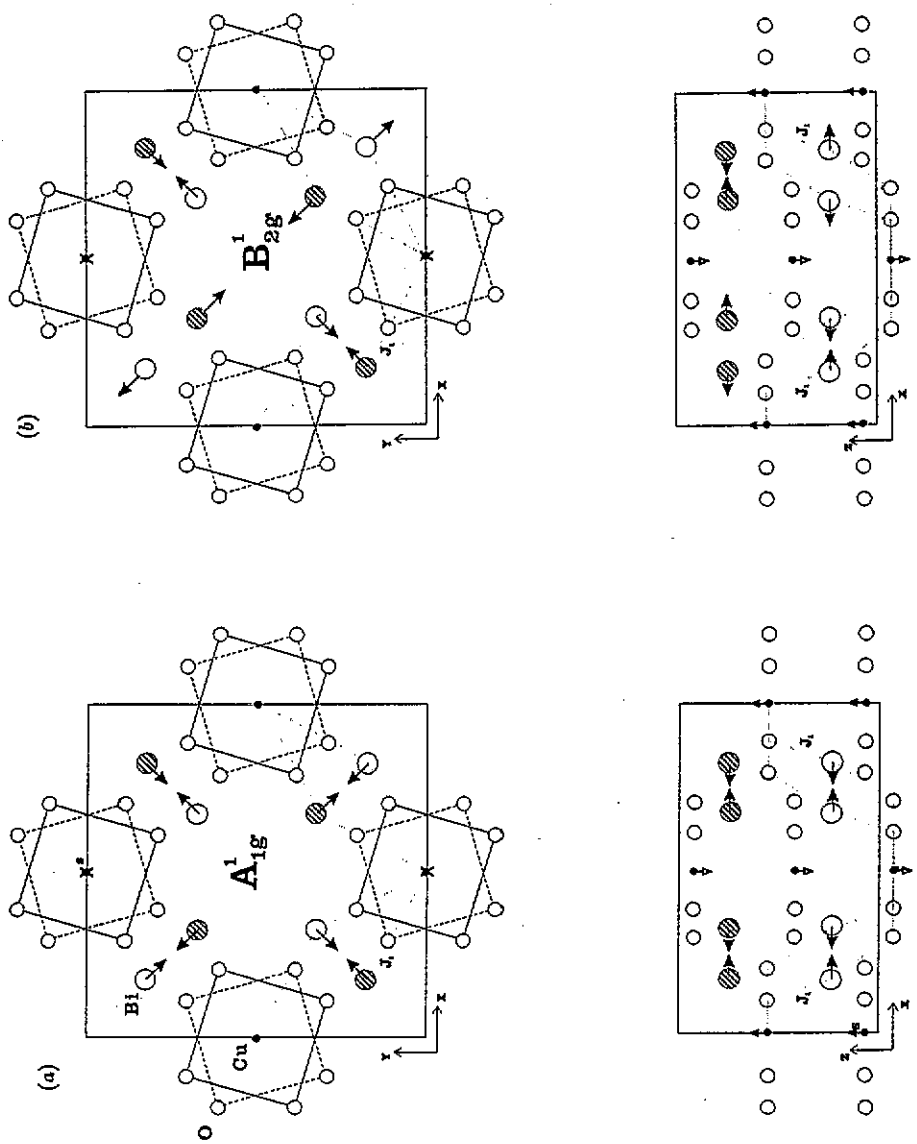

Figure 3. A_{1g} (*a*) and B_{2g} (*b*) normal-mode displacements and superexchange pathway J_1 (J_1 is denoted by dashed line, spin is oriented along z axis).

The Raman spectra given in figure 1 allow us the possibility of studying temperature dependencies of phonon modes, too. The A_{1g} phonon modes intensities versus temperature are presented in figure 2(*a*). As can be seen from figure 2(*a*), the 128 cm^{-1} and 135 cm^{-1} modes exhibit a strong anomaly near the Néel phase transition temperature. While the temperature is decreasing, the intensities of these two phonon modes are slowly increasing, then they fall at a local minimum at T_N. Finally, there is a strong increase again below T_N. Other modes do not show the same behaviour, but their intensities have changing slopes at T_N.

The temperature dependencies of the B_{2g} phonon mode intensities are shown in figure 2(*b*). As can be seen from figure 2(*b*), there is no anomaly around the Néel phase transition point. The intensities of the 82 cm^{-1} and 132 cm^{-1} modes are decreasing down to the lowest temperature we observed at 10 K. The intensities of the other two modes of the same symmetry show different temperature dependencies. Their intensities are increasing up to the temperatures around 70–100 K and then they are decreasing until 10 K.

The effect of spin-dependent phonon intensities has been discussed in the ferromagnetic semiconducting spinels $CdCrS_4$ and $CdCrSe_4$ by Steigmeier and Harbeke [12]. In order to explain this phenomenon, Suzuki and Kamimura [13] proposed a mechanism of the d-electron–phonon scattering process. However, it was shown in [14–16] that the increase of the integrated phonon Raman intensity below the Curie temperature depends on the wavelength of the exciting light. We will discuss our results in the light of the theory of Suzuki and Kamimura [13], and presented symmetry consideration.

The normal coordinate analysis and lattice dynamical calculation for Bi_2CuO_4, together with the mode assignment, were given in [8]. We recall here that modes at 128 cm^{-1} (A^1_{1g}) and 82 cm^{-1} (B^1_{2g}) originate from in-plane Bi–Bi motion, the mode at 135 cm^{-1} (A_{1g}) originates from translational vibration of the CuO_4 planes along the z axis, and all other modes come from different oxygen motion [8]. The A^1_{1g} and B^1_{2g} normal-mode displacements in xy and xz projections are shown in figure 3(*a*) and (*b*), respectively.

According to the theory of Suzuki and Kamimura [13], the three patterns of the integrated phonon intensity as a function of the temperature is found, depending on the R/M ratio: R and M are Raman tensors associated to the spin-independent and spin-dependent terms. Comparison between our results and that of the figure 1(*b*) in [10], for the antiferromagnetic case, which corresponds to $0 < R/M < 1$, gives good consistency indeed.

The different behaviour of the phonon intensities between A_{1g} and B_{2g} modes we explained using symmetry arguments. The pathways through which the superexchange propagates, together with normal-mode displacements, are presented in figure 3 (J_1 denoted by the dashed line). The careful inspection of the symmetry results presented in this figure led us to the conclusion that A^1_{1g} normal mode acts in-phase concerning the J_1 superexchange, while the B^1_{2g} normal mode acts out-of-phase. Consequently, the B^1_{2g} normal mode does not influence the change of superexchange as A^1_{1g} does. The same argument holds for all other modes of these symmetries. Unfortunately, we could not compare our results with other antiferromagnetic materials due to, as far as we know, lack of similar experimental results in the literature.

4. Conclusion

On the basis of the experimental results and symmetry analysis of the magnetic space groups for two proposed spin orientations in Bi_2CuO_4, we concluded that the magnetic moments in this oxide have z axis orientation. The phonon-mode temperature dependencies for A_{1g} symmetry show a strong anomaly near the Néel phase transition temperature.

Acknowledgments

We thank A Revcolevschi for providing us with the Bi_2CuO_4 single crystal. One of us (ZVP) acknowledges the Alexander von Humboldt foundation (Federal Republic of Germany) for donating us the closed-cycle cryostat used here. This work was supported by the Serbian Ministry of Science and Technology under Project 0104.

References

[1] Boivin J C, Tomas D and Tridot S 1973 *C. R. Acad. Sci., Paris* C **276** 1105
[2] Konstantinović J, Stanišić G, Ain M and Parette G 1991 *J. Phys.: Condens. Matter* **3** 381
[3] Ong E W, Kwei G H, Robinson R A, Ramakrishna B L and von Dreele R B 1990 *Phys. Rev.* B **42** 4255
[4] Yamada K, Takada K, Hosoya S, Watanabe Y, Endoh Y, Tomonaga N, Suzuki T, Ishigaki T, Kamijama T, Asano H and Izumi F 1991 *J. Phys. Soc. Japan* **20** 2406
[5] Konstantinović M J, Popović Z V, Dević S D, Revcolevschi A and Dhalenne G 1992 *J. Phys.: Condens. Matter* **4** 7913
[6] Ain M, Dhalenne G, Guiselin O, Hennion B and Revcolevschi A 1993 *Phys. Rev.* B **47** 8167
[7] Popović Z V, Kliche G, Cardona M and Liu R 1990 *Phys. Rev.* B **41** 3824
[8] Popović Z V, Kliche G, Konstantinović M J and Revcolevschi A 1992 *J. Phys.: Condens. Matter* **4** 10085
[9] Dhalenne G, Revcolevschi A, Ain M, Henion B, Andre G and Parette G 1991 *Cryst. Prop. Prep.* **11** 36
[10] Cracknell A P 1969 *J. Phys. C: Solid State Phys.* **2** 500
[11] Bradley C J and Cracknell A P 1972 *The Mathematical Theory of Symmetry in Solids* (Oxford: Clarendon)
[12] Steigmeier E F and Harbeke G 1970 *Phys. Kondens. Matter* **12** 1
[13] Suzuki N and Kamimura H 1973 *J. Phys. Soc. Japan* **23** 967
[14] Koshizuka N, Yokoyama Y and Tsushima T 1976 *Solid State Commun.* **18** 1333
[15] Iliev M, Güntherodt G and Pink H 1978 *Solid State Commun.* **27** 863
[16] Iliev M N, Anastassakis E and Arai T 1988 *Phys. Status Solidi* B **86** 717